Further Test and Validation of Saturation-recovery T1 MRI Measurement for Imaging Absolute CBF Change

X. Wang[1], X-H. Zhu[1], Y. Zhang[1], and W. Chen[1]
[1]Center for Magnetic Resonance Research, Department of Radiology, University of Minnesota, Minneapolis, Minnesota, United States

Introduction: The feasibility for imaging and quantifying absolute change of cerebral blood flow (CBF) using saturation-recovery T_1 MRI approach has been previously demonstrated using rat ischemia (decreasing CBF) and hypercapnia (increasing CBF) models at 9.4T[1]. Briefly, the water exchange between the capillary and brain tissues through the blood perfusion will affect the apparent water T_1, thus, its change can be applied to determine the CBF difference (ΔCBF) between the two conditions. However, the questions were that: 1) whether the large vessel inflow effect would contribute to T_1/R_1 change and therefore affect CBF quantification? 2) If the transit time of blood flow could significantly bias the T_1/R_1 measurement for determining ΔCBF in rat brain at 9.4T? Two experiments were designed to address these questions. One was the use of diffusion-weighted image to suppress the large-vessel inflow effect, by thus comparing the R_1 values with and without diffusion gradients and its difference (ΔR_1). The other was using slab saturation preparation with varied thickness to spatially manipulate blood transit distance, thus, testing the effect of blood transit time on ΔCBF measurement.

Theory: The previously described T_1 (or $R_1 = 1/T_1$) images were measured by the combination of global brain saturation preparation and EPI readout after varied saturation-recovery time (T_{SR}). The relationship of CBF and R_1 can be formulated by [2-3]: $R_1^{app} = R_1^{int} + CBF/\lambda$, where R_1^{app} is the apparent R_1, R_1^{int} stands for intrinsic R_1 which is a constant and insensitive to physiology change, λ (=0.9ml/g) is the blood-tissue water partition coefficient; thus, $\Delta CBF \approx \lambda \times \Delta R_1^{app}$. The diffusion weighting is determined by b factor = $(\gamma \cdot G \cdot \delta t)^2 \cdot (T - \delta t/3)$, where γ is the gyromagnetic ratio, G and δt are the magnitude and duration of diffusion gradient, T is the delay between the bipolar gradients.

Material and MRI method: The MRI experiments were carried out in a horizontal 9.4T animal magnet with an 8-shape surface coil (2.8cm×2cm). Eight male rats were used for conducting ten hypercapnia experiments for testing large vessel inflow effect using diffusion-weighting MRI, and another group of six rats were used to conduct nine hypercapnia experiments for testing transit time effect with varied slab saturation thickness. The animal anesthesia was maintained at 2% isoflurane. The hypercapnia was induced by switching to an inhalation bag with mixed gases (6% CO_2, 34% O_2, 58% N_2O and 2% isoflurane) for 20-30 minutes. All the R_1^{app} image measurements were acquired before (i.e., normocapnia or control) and during stable hypercapnia condition, when the animal physiology (monitored during the entire experiment) was within a normal range. Gradient echo EPI (TE=21ms; FOV=3.2×3.2cm; image matrix=64×64; 1 mm thickness) combined with the saturation-recovery preparation was used for imaging T_1^{app} with nine varied T_{SR} of 0.008, 0.1, 0.2, 0.3, 0.4, 0.5, 1.4, 3 and 10 s. Three b factors (0, 518, 1019 s·mm^{-2}) were achieved by adjusting the diffusion gradient strength with δt = 2.5 ms and T = 3.6ms. For varied thickness slab (0.5cm and 1cm) saturation preparation studies, the EPI slice was located in the middle of saturated slab. Slab saturation was achieved through a BISTRO pulse train combined with slice-selection gradients. ROI data taken from the rat somatosensory cortex were used to perform the R_1 regression analysis and determine R_1^{app} and ΔR_1^{app}. MRI data analysis was performed using the STIMULATE software package and the Matlab software package. R_1^{app} and ΔR_1^{app} maps were generated with two-dimensional median filtering on a pixel by pixel basis. One way ANOVA and paired t-test were used for statistic analysis.

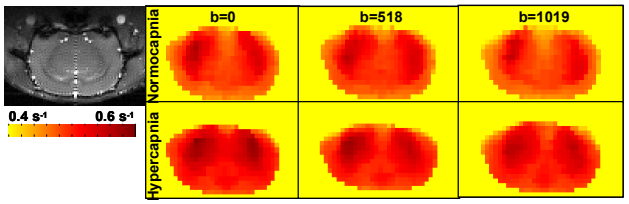

Figure 1 Anatomic coronal image and R_1^{app} maps with and without bipolar diffusion gradients under both normocapnia and hypercapnia conditions in a representative rat.

Table 1 Summary of R_1^{app} and delta R_1^{app} values with and without bipolar diffusion gradients under both normocapnia and hypercapnia conditions.(n=10)

	Normocapnia R_1^{app} (s^{-1})			Hypercapnia R_1^{app} (s^{-1})			Delta R_1^{app} (s^{-1})		
	b=0	b=518	b1019	b=0	b=518	b1019	b=0	b=518	b1019
Mean	0.4806	0.4791	0.4810	0.5058	0.5017	0.4982	0.0252	0.0226	0.0172
Std	0.0063	0.0067	0.0071	0.0079	0.0073	0.0070	0.0072	0.0059	0.0053
One-Way ANOVA	p = 0.93			p = 0.12			p = 0.06		

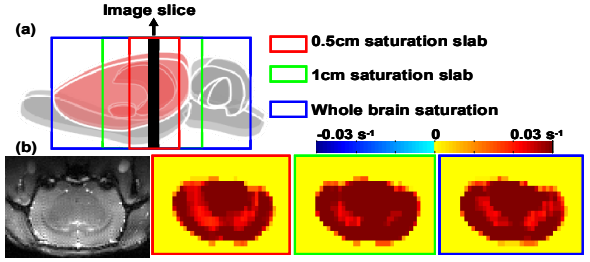

Figure 2 (a) Schematic graph for varied saturation preparation region. (b) Anatomic coronal image and Δ R_1^{app} maps between normocapnia and hypercapnia conditions with varied saturation slabs in a representative rat. The outline color of Δ R_1^{app} maps are consistent with schematic graph.

Results: Figure 1 shows anatomic image and R_1^{app} maps obtained with and without bipolar diffusion gradients under both normocapnia and hypercapnia conditions in a representative rat. The whole brain R_1^{app} elevates during the hypercapnia due to the global CBF increase. There is a similar spatial pattern of R_1^{app} maps under different b factor diffusion weightings for both normocapnia and hypercapnia conditions. Table 1 summarizes the comparison results, indicating a negligible effect of diffusion gradients on the R_1^{app} and ΔR_1^{app} measurements. Figure 2a shows schematic illustration of varied saturation regions. Figure 2b shows the anatomic image and ΔR_1^{app} difference maps between normocapnia and hypercapnia R_1^{app} images with varied saturation slabs in a representative rat. It indicates that both magnitude and pattern change of ΔR_1^{app}s with three different saturation preparations are similar regardless of different slab saturation thickness. Besides the nine T_{SR} points (0.008, 0.1, 0.2, 0.3, 0.4, 0.5, 1.4, 3 and 10 sec) fitting for R_1^{app} analysis, four points (0.5, 1.4, 3 and 10sec) fitting of the identical data set was performed to purposely ignore the magnetization contribution of initial saturation-recovery period of ≤ 400ms, which is comparable to the blood transit delay time in the rat brain. Surprisingly, almost identical results were found among ΔR_1^{app} values (0.0217 s^{-1} vs.0.0206 s^{-1} for 0.5cm saturation slab, 0.0272 s^{-1} vs. 0.0264 s^{-1} for 1cm saturation slab, 0.0211 s^{-1} vs. 0.0215 s^{-1} for whole brain saturation) based on nine points fitting approach compared to four points fitting approach despite the fitted R_1^{app} values being systematically different.

Discussion and conclusion: The diffusion gradient tends to suppress the macrovascular signal and large vessel in-flow effect, especially when the high b factor is applied [4-5]. Our results indicate no statistical difference between R_1^{app} and ΔR_1^{app} values in the presence and absence of diffusion weighting gradients under both normocapnia and hypercapnia conditions. This finding suggests that the macrovascular inflow effect does not dominate the R_1^{app} measurement and its effect on quantifying ΔCBF is negligible. Otherwise a persistent decrease in R_1^{app} is expected when the b factor increases. Moreover, the short T_2 in venous blood at high field (~9 ms at 9.4T) could further minimize the macrovascular in-flow contribution from the venous side when TE=23 ms was used in EPI in this study. By varying the saturation slab thickness, one could expect to see the dependence of R_1^{app} on the varied transit distance if the blood transit time indeed affects R_1^{app}. For example, the blood transit distances are about 2mm, 4.5mm and >9.5mm when the saturation slabs are 0.5cm, 1cm and the global brain saturation respectively. One would expect that R_1^{app} value could be largest when the 0.5cm saturation slab is applied because of its shortest transit distance. Our results, however, did not show statistic difference in R_1^{app} and ΔR_1^{app} among three distinct slab saturation widths. The ΔR_1^{app} values derived from four points fitting also show no statistic difference with nine points (paired t-test results: p = 0.1, 0.2, 0.72 for 0.5cm, 1cm and global brain saturation slab), indicating that the ΔR_1^{app} values are consistent disregard of the different fitting approaches. This result suggests that transit delay time might not be a major concern for imaging ΔCBF based on the ΔR_1^{app} measurement. Lastly, the calculated CBF increase induced by hypercapnia was ~1.25ml/g/min, which is consistent with literatures under similar condition. In conclusion, overall results from this study reveal that the large vessel inflow effect and transit delay time have negligible effects on quantifying the CBF change based on the saturation-recovery T_1 MRI measurement.

Acknowledgments: NIH grants: NS41262, NS57560, P41 RR08079 and P30NS057091; and the Keck foundation.

References: 1. Wang et.al *ISMRM proceedings*, 1481, 2009. 2**.** Kwong et al. *MRM*, 1995; 3. Kim, *MRM*, 1995;, 4. Song et al. *MRM* 1996; 5.Yacoub et al. *MRI*, 2008.